Studies of the thermal dissolution process of the Suzuki phase of the Eu^{2+} ion in KBr single crystals by analysis of photoacoustic signals

2003 J. Phys.: Condens. Matter 15 6889

(http://iopscience.iop.org/0953-8984/15/40/024)

INSTITUTE OF PHYSICS PUBLISHING JOURNAL OF PHYSICS: CONDENSED MATTER

J. Phys.: Condens. Matter **15** (2003) 6889–6898 PII: S0953-8984(03)64552-2

Studies of the thermal dissolution process of the Suzuki phase of the Eu^{2+} ion in KBr single crystals by analysis of photoacoustic signals

E V Mejía-Uriarte[1], R Castañeda-Guzmán[1], M Villagrán-Muniz[1], E Camarillo[2], J Hernández A[2], H Murrieta S[2] and M Navarrete[3]

[1] Centro de Ciencias Aplicadas y Desarrollo Tecnológico, Laboratorio de Fotofísica, Universidad Nacional Autónoma de México, AP 70-186, CP 04510 México, DF, Mexico
[2] Instituto de Física, Universidad Nacional Autónoma de México, AP 20-364, CP 01000 México, DF, Mexico
[3] Instituto de Ingeniería, Coordinación de Ingeniería Mecánica Térmica y Fluidos, Universidad Nacional Autónoma de México, AP 70-543, México, DF, Mexico

Received 5 June 2003
Published 26 September 2003
Online at stacks.iop.org/JPhysCM/15/6889

Abstract

An experimental investigation of the thermal behaviour of the dissolution process of the Suzuki phase (SP) by continuous heating (1 °C min^{-1}) of KBr:Eu^{2+} crystals is reported in this work. The thermal profiles were determined by the correlation functions between subsequent photoacoustic (PA) signals registered during the dissolution process. The behaviour of the thermal profile is directly related to the absorption coefficient of the Eu^{2+} ion in precipitated states that are present in the crystal. The PA signal is detected as a consequence of the non-radiative processes that take place after the excitation of the low-energy band of the Eu^{2+} ion by means of a focused laser pulse at 355 nm. The results obtained by this method are compared with those simultaneously obtained by the photoluminescence (PL) technique. The samples were heated from room temperature to 205 °C. The PA signal and PL spectrum were obtained every 6 °C. The temperature range of the SP dissolution process was from 77 to 115 °C. These results are in agreement with those obtained by the PL technique and with the data reported in the literature.

1. Introduction

In general, the precipitated phases in alkali halides doped with divalent cations can take different structures. A great deal of work has been reported on the optical properties of europium-doped alkali halides [1–4], particularly the precipitated states. Suzuki performed an extensive x-ray diffraction study on the nature of the metal ion impurities precipitated in the alkali halides. The results of these studies indicate that in the NaCl–$CdCl_2$ system, the Cd^{2+} ions segregate on the {100} planes, producing a metastable phase with a stoichiometry 6NaCl–$CdCl_2$. The crystalline structure is an fcc lattice, with a lattice parameter twice that of the original matrix;

this is known as a Suzuki-type precipitated phase (SP) [5–9]. The presence of an SP can be detected by means of optical absorption [1], x-ray diffraction [7–9] and PL techniques [10, 11].

The absorption spectrum of Eu^{2+} ions consists of two broad absorption bands. These are attributed to transitions from the $4f^7(^8S_{7/2})$ ground state of Eu^{2+} into e_g (high-energy absorption band) and t_{2g} (low-energy absorption–emission band) states of the $4f^65d$ configuration in an octahedral crystal field. By excitation with light, in either of these two bands, there is only one emission band, the position of which depends on the alkali halide. Also, the position of this emission band depends on the Eu^{2+} ion concentration and the thermal history of the crystal [11]. In the case of KBr:Eu^{2+} this spectrum, for a quenched sample, has peaks around 420 nm due to europium–vacancy complexes or free dipoles. Annealing of quenched samples at temperatures below 100 °C produces the growth of an emission band (peaking at 433 nm in KBr:Eu^{2+} crystals), that has been related to the presence of Suzuki-type precipitates [10].

The average size of the SP precipitates of the Eu^{2+} ion depends on the impurity concentration, crystal preparation conditions and, in particular, on the cooling rate. The precipitate size increases with an increase in impurity concentration and with a decrease in the cooling rate. To our knowledge there are no reports of the average precipitate size of SP in KBr:Eu^{2+}. In alkali halide crystals doped with other divalent impurities and cooled after growing to room temperature (RT) at a rate of 200 °C s^{-1}, SP regions of around 20 nm in diameter have been observed, while for slowly cooled crystals, regions above 100 nm in diameter have been obtained [12–14].

In this paper, a comparison between the results obtained by photoacoustic (PA) and photoluminescence (PL) techniques during a dynamical thermal dissolution process is developed.

The temperature range at which thermal dissolution of SP occurs is determined by correlation analysis of the PA signals. The behaviour of the thermal profile is directly related to the absorption coefficient of Eu^{2+} ions in precipitated states that are present in the crystal.

2. Photoacoustic

The PA effect is related to the phenomenon of the generation of acoustic waves in a medium after interaction with modulated or pulsed light, and was discovered by Bell in 1880 [15, 16]. Acoustic waves generated by the interaction with laser pulses in condensed matter have been widely used for materials characterization [17–23]. One important property of this phenomenon is that the resultant PA signal depends on the absorption properties and the thermoelastic parameters of the sample. In general, different deexcitation mechanisms occur, such as thermal and non-thermal (fluorescence, photochemistry, photoconductivity, etc) deexcitation channels.

The heat produced by deexcitation processes that take place in the sample, after laser pulse excitation, is detected as a PA signal. The foregoing discussion suggests that the radiative and non-radiative processes can be studied as PL and PA signals respectively.

Assuming that the energy released as heat from non-radiative (thermal) processes can be expressed as

$$E_{\text{heat}} = E_0\left[1 - \sum_i \xi_i\right], \tag{1}$$

where E_0 is the energy absorbed in the system and ξ_i are the conversion efficiencies of several non-thermal deexcitation channels. Since the PA signal is proportional to E_{heat}, it can, in general, be written as

$$S = S_0\left[1 - \sum_i \xi_i\right], \tag{2}$$

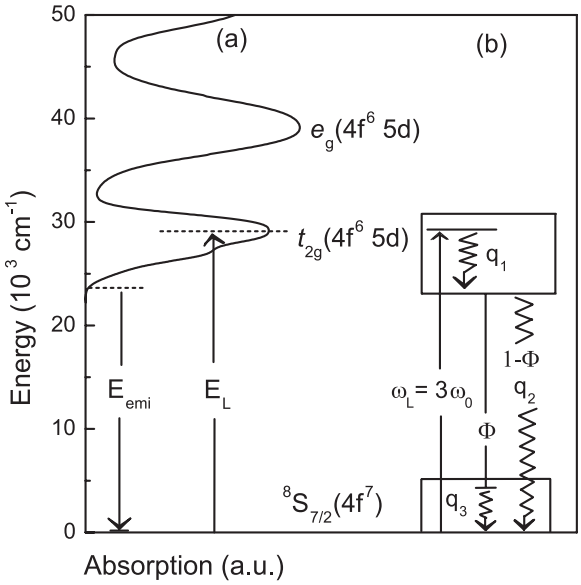

Figure 1. (a) The absorption bands of Eu^{2+} in KBr, showing the coincidence with the third ($3\omega_0$) harmonic of the Nd:YAG laser. (b) A schematic energy diagram indicating the different contributions to the PA and PL signals.

where S_0 is the S signal when only the thermal deexcitation mechanisms are present. For Eu^{2+} in KBr crystals, the non-radiative processes from Eu^{2+} are registered as S signals [16].

It is known that the KBr host is optically transparent. Therefore, only the Eu^{2+} impurities absorb the light. The two Eu^{2+} absorption bands are shown in figure 1(a); under our experimental conditions, only the low-energy band was excited. The excitation of this band was carried out by the third harmonic of a Nd:YAG laser ($3\omega_0$, $\lambda = 355$ nm). After pulsed excitation, the luminescence decays exponentially after a fast rise, coincident with the excitation time. The emission band and the S signal corresponding to $t_{2g} \rightarrow 4f^7$ transitions were detected simultaneously. Additionally, illumination using frequencies out of the Eu^{2+} absorption bands of the Nd:YAG laser at 532 nm gives no detectable PA signal. Therefore the signal detected after excitation at $3\omega_0$ can be unequivocally related to processes originating after Eu^{2+} absorption.

Figure 1(b), shows the t_{2g} excitation band and relaxation processes. The non-radiative relaxation within this level gives a thermal contribution q_1. The relaxation from the bottom of the lower excited level to the $4f^7$ ground level is assumed to be luminescent with a quantum efficiency Φ. This radiative process is followed by non-radiative relaxation within the ground state giving a thermal contribution Φq_3, while on the other hand, the non-radiative channel also gives a contribution $(1 - \Phi)q_2$ [24].

According to these processes, the PL spectrum and S signal may be expressed as:

$$\mathrm{PL}(3\omega_0) = C_\mathrm{L}\Phi N_\mathrm{a}(3\omega_0) \tag{3}$$

$$S(3\omega_0) = C_\mathrm{P}[q_1 + (1 - \Phi)q_2 + \Phi q_3]N_\mathrm{a}(3\omega_0) \tag{4}$$

where $N_\mathrm{a}(3\omega_0)$ is the number of absorbed photons and C_L and C_P are instrumental constants.

The absorbed photons are used to excite a number of Eu^{2+} ions, the number being proportional to the absorption coefficient $\alpha_{\mathrm{Eu}}(\upsilon)$ of each type of europium precipitated state. Subsequently equation (4), may be expressed in the following form:

$$S = K\alpha_{\mathrm{Eu}}(\upsilon) \tag{5}$$

showing a clear relationship with the optical absorption coefficient $\alpha_{Eu}(\upsilon)$ of the Eu^{2+} ion, which is known to be related to the aggregation–precipitation state υ of the europium ions [1], and K is a proportionality constant. Thus, in a deexcitation process the PA signal is directly related to the absorption [16, 24].

The differences among the S signals, arising from the SP and europium–vacancy dipoles, are then due to the changes in the crystalline field interactions with the $4f^65d$ excited state of the Eu^{2+} ion. The same behaviour and dependence is obtained for the PL spectrum.

3. Signal analysis

Correlation techniques are used for the electronic signals because they allow evaluations to be carried out in real time without the need for expensive electronic processing and they guarantee less sensitivity to the noise. The autocorrelation technique is suitable for extracting possible patterns present in the signals being considered. Furthermore, it allows the evaluation of the changes in the signals during a thermal process. The delay at which the absolute maximum is exhibited corresponds to the temperature changes between the signals on which the correlation function is computed [25].

$S(T_n)$ is the PA time history recorded at a specific temperature T_n, which contains phenomenological information from the material. The correlation between functions $S(T_1)$ and $S(T_{1+i})$ will reveal changes occurring in the sample at the temperature interval $T_{1+i} - T_1$. So, the correlation of two real signals is given by:

$$c_S(T_1, T_{1+i}) = \langle S_{T_1} S_{T_{1+i}} \rangle. \tag{6}$$

Furthermore, the correlation between $S(T_1)$ and $S(T_{1+i})$ will be 1 if both functions are the same, but less than 1 if any change occurs between them. Then we can built a function $N_S(T)$ with a maximum correlation value or correlation coefficient for each temperature, which represents the mean square value [18, 25]. By means of the ensemble of the correlation coefficients $N_S(T)$ as a function of temperature, it is possible to find the behaviour of the thermal profile from Suzuki phase dissolution processes by continuous heating [20].

We performed another correlation analysis of the PA signals. The correlation between successive signals $S(T_i)$ and $S(T_{1+i})$ can show the range of temperature over which the dissolution process begins and finishes. This analysis makes evident the shift between the different PA signals and gives little weight to the amplitude of the signal [19].

Therefore, we can built a new function $N'_S(T)$ with a correlation coefficient (from the correlation between successive signals) for each temperature. This new $N'_S(T)$ ensemble as a function of temperature shows the range of the SP dissolution process [18–20].

4. Experimental set-up

The KBr and KBr:Eu^{2+} crystals used in this study were grown by the Czochralski method. Single crystals of potassium bromide doped with divalent europium were grown in our laboratory using the Czochralski method under a controlled atmosphere of dry argon at 40 Torr in order to minimize contamination by OH, H_2O and oxygen which are present in air and could affect the solubility and precipitation phenomena. We used Merck Suprapur products. The crystals were slowly cooled to RT inside the furnace. Eu^{2+} was introduced by adding $EuBr_2$ powder to the melt, which was previously reduced from $EuBr_3{\cdot}6H_2O$ using standard techniques. This method has been used in our previous works [1–3, 10, 11].

Crystal samples were heated for about 1 h at 500 °C and subsequently quenched by dropping them onto a copper block at RT, in order to dissolve the europium aggregates and precipitates. Then the samples were subjected to suitable thermal treatments in order to produce Suzuki-type europium precipitates; they were annealed at 80 ± 3 °C inside a standard furnace

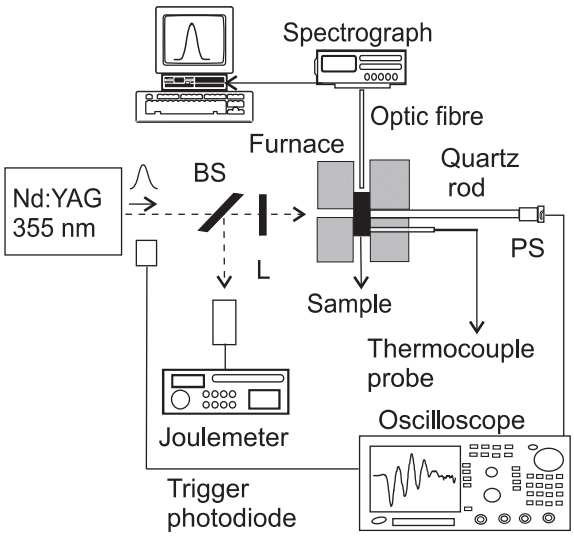

Figure 2. Schematic diagram of the simultaneous dynamical measuring system employed to obtain the behaviour of KBr:Eu^{2+} crystals during thermal dissolutions: BS = beam splitter, L = focusing optics, PS = piezoelectric sensor.

for 16 weeks. The impurity concentration was calculated by using the optical absorption coefficient of the high-energy absorption band recorded at RT [2]. The absorption spectra were obtained with a Milton–Roy spectrophotometer. The samples had a rectangular shape with area 1 cm^2 and thickness 1–1.95 mm. Samples with concentrations of about 220–270 ppm of Eu^{2+} were selected for the experiments. The emission band peak of the KBr:Eu^{2+} in quenched samples was at 423 nm; after the annealing at 80 °C the emission band peak was shifted to 433 nm and was detected with a Perkin-Elmer model 650-10S fluorescence spectrophotometer.

A block diagram of the dynamical measuring system is shown in figure 2. To obtain the S signal and PL spectra, the sample was illuminated with a Q-switched Nd:YAG laser (355 nm, 20 ns pulse width, 10 Hz) with an output pulse energy ranging typically 0.68 mJ. The diameter of the irradiated spot was about 1 mm. Laser energy variations were measured through a beam splitter by a Joulemeter, with a RjP-700 display from Laser Precision Corp. The sample was held between two electrically heated plates connected to a temperature control (Ω RcK-Rex P90). The sample temperature was measured with a chromel–alumel thermocouple attached to the sample. A long Pyrex rod ($\phi = 5$ mm, $l = 17$ cm) was used to carry the ultrasonic signals outside the furnace to a piezoelectric sensor (150 kHz). The signal was recorded by a 500 MHz digital oscilloscope (Tektronix TDS 524), at a sampling rate of 100 M samples s^{-1}. The light emitted from the sample was collected using an optical fibre connected to a spectrograph (Ocean Pacific 2000). Each sample was heated from RT to 205 °C at a rate of 1 °C min^{-1}, while the pulsed beam was focused onto the sample to excite the low-energy europium absorption band and to generate the acoustic emission. During heating, the emission spectrum and S signal were simultaneously recorded every 6 °C. The experiments were performed with five samples in order to ensure reliability of the results.

5. Experimental results and discussion

Figure 3 shows some of the PA signals for different temperatures; changes in amplitude, phase and form of the PA signal can be clearly observed. The correlation coefficients $N_S(T)$ and $N'_S(T)$, as a function of temperature, are associated with the dissolution process of the SP.

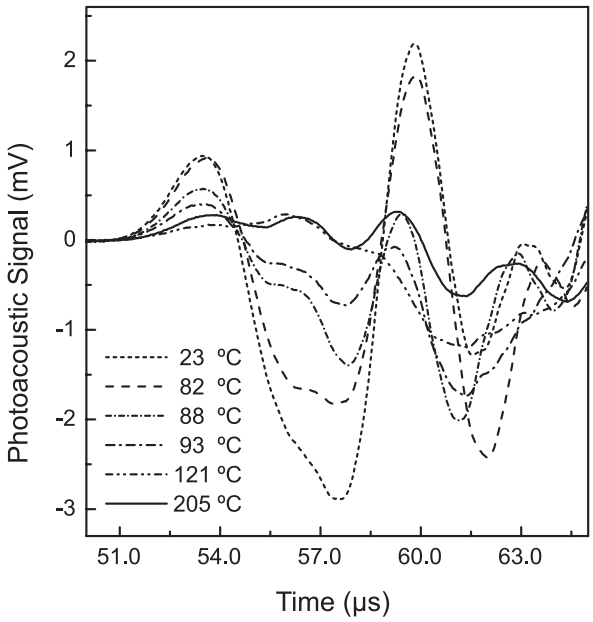

Figure 3. Photoacoustic signals for several temperatures; before, during and after the dissolution process of the SP.

The ensembles $N_S(T)$, as a function of temperature in figure 4, show the temperature profile for two KBr:Eu^{2+} samples. Figure 4(a) shows the profile for a sample with Eu^{2+} in the form of free dipoles (quenched sample). The amplitude of the PA signal decreases with increase of the temperature due to changes in the bulk; this is represented by a monotonic decrease in the $N_S(T)$ ensemble. The same behaviour was observed in all the KBr:Eu^{2+} samples in the form of free dipoles that we have tested. Therefore, this does not demonstrate any dissolution process from aggregated–precipitated states, as expected from a quenched sample. Also, considering the definition in equation (5), as the europium ions are in free dipoles and the S signal is in turn proportional to the absorption coefficient, the behaviour is expected to be almost constant with the increase in temperature. This was verified by the emission spectra; the emission band peak (423 nm) had a shift of <2 nm.

Figure 4(b) shows a dissolution thermal process profile for the sample in the SP. This profile is associated with the precipitated states by means of its $\alpha_{Eu}(\upsilon)$, where υ is a parameter that describes the crystalline environment of the Eu^{2+} ions. We represent an **A** state by $\alpha_{Eu}(\upsilon_A)$, where υ_A represents the precipitated state in the SP; in this precipitated phase the next nearest neighbour (NNN) dipole positions are more stable than the next nearest (NN) ones [26]. Thus the S signal is detected as a function of the $\alpha_{Eu}(\upsilon_A)$ for different T_i: as the changes are not significant, the $N_S(T)$ profile only presents a slight slope until 77 °C; later the profile exhibits a jump until it reaches a temperature of 94 °C, which presents a new **B** state with υ_B, where υ_B represents the new crystalline environment due to changes in the interaction of the crystalline field with $4f^6 5d$ excited states of the Eu^{2+} ions, when the SP precipitates have been dissolved. In this new state the europium–vacancy dipoles and small precipitates that come from the dissolution of the Suzuki phase are present. The discontinuity between states **A** and **B** is about 40% of the $N_S(T)$. This jump might be due to the dispersion of Eu^{2+} from SP precipitates. The above-mentioned behaviour was in agreement with the wavelength shift observed in the PL spectra, obtained simultaneously.

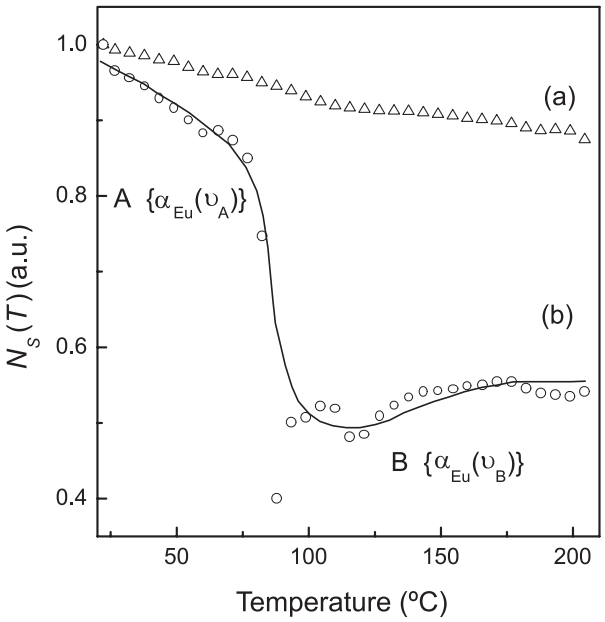

Figure 4. The $N_S(T)$ obtained from S signal sequences as a function of temperature for: (a) KBr:Eu^{2+} (270 ppm) quenched sample (△); (b) KBr:Eu^{2+} (250 ppm) sample in SP (○).

The $N'_S(T)$ ensemble is used to estimate the range of temperatures that characterize the jump. In order to make a comparison between the different europium states in figure 5 two profiles are shown: in figure 5(a) KBr:Eu^{2+} (quenched sample) does not show a change in the profile; in figure 5(b) the profile of the KBr:Eu^{2+} sample in SP reveals a range of temperatures of about (77–115) $\pm$ 3 °C, where the dissolution presumably was carried out, this result is compared with that reported by Aguilar *et al* [10] who gave a range 80–120 °C where the thermal dissolution of the SP was carried out.

Figure 6(a) displays the results obtained for the position of the emission band for different temperatures during the SP dissolution process. The PL spectrum registered displays one broad band peak centred at 433 nm, which is the main characteristic of KBr:Eu^{2+} crystals in SP form at RT. When the temperature increases, the peak position shifts to shorter wavelengths—to about 423 nm due to crystalline field interactions. This emission band can be understood as a coexistence of the Eu^{2+}–vacancy complexes and small precipitates that come from the dissolution of the SP.

In figure 6(b) the evolution of the emission band intensity should be noted. There is an increase in the band intensity as the temperature increases, which might be due to the change in precipitation size conditions; these changes might be in turn proportional to the light scattering produced during the dynamical thermal process.

This process was monitored in real time; therefore the behaviour of the emission spectra intensity is different from that reported by Aguilar *et al* [10] (a process in quasi-thermodynamic equilibrium), where there is no change in the intensity and the emission bandwidth for temperatures up to $\sim$70 °C is constant.

In this work we find that there are variations of the emission bandwidth and a slight decrease of the intensity up to 155 °C. Later the emission intensity increases quickly, as can be seen in figure 6(b). This can be explained in terms observations of the dynamical heating process, because the precipitates are smaller and there is less scattering of the light.

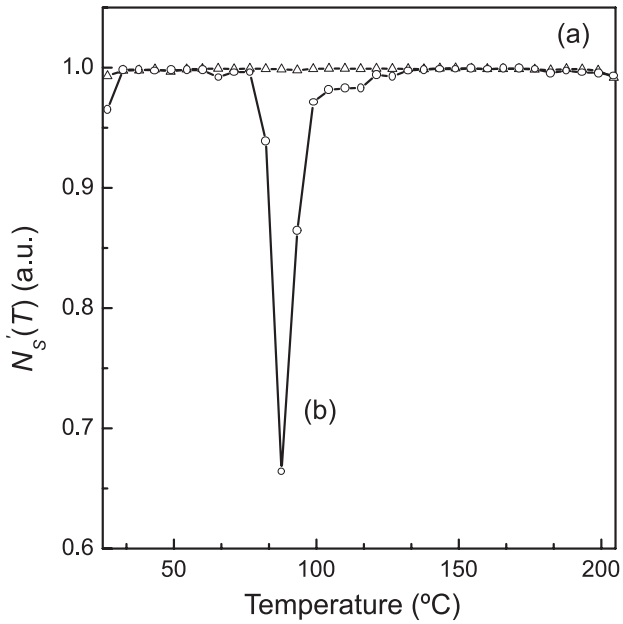

Figure 5. The behaviour of $N_S'(T)$ as a function of temperature: (a) KBr:Eu^{2+} (270 ppm) quenched sample (–△–); (b) KBr:Eu^{2+} (250 ppm) sample in SP (–O–).

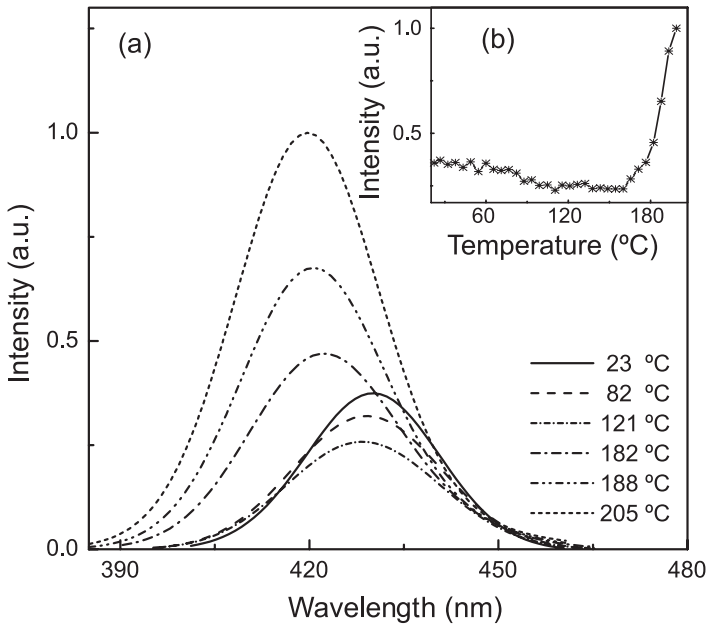

Figure 6. (a) Eu^{2+} emission spectra at different temperatures. (b) Emission intensity (area under the curve) as a function of temperature.

The experimental results obtained with the PA technique show good agreement with those obtained by the PL technique and with the work previously reported [10].

6. Conclusions

Eu^{2+} ion precipitates have been determined through their absorption coefficient during dissolution processes by continuous heating. The differences between the $\alpha_{Eu}(\upsilon)$ are due to changes in the crystalline field interaction with $4f^6 5d$ excited states of the Eu^{2+} ions in the different precipitates. The absorption behaviour was registered by means of the recording of PA signals generated from non-radiative processes. Therefore, the changes in the S signal as function of temperature are correlated with the absorption coefficient of each type of europium precipitated state.

To obtain the thermal profiles we used two correlation functions, whose coefficients $N_S(T)$ and $N'_S(T)$ were assembled as a function of temperature. The first profile shows the absorption behaviour and its changes from RT to 205 °C. The second profile shows the range of temperatures (77–115) $\pm$ 3 °C where the dissolution of the Suzuki phase occurred. The last result is in agreement with the literature. Photoacoustic monitoring in non-stationary thermal conditions of Suzuki-type europium precipitates in KBr crystals during the thermal dissolution process has been demonstrated. This procedure determines in real time the temperature range of SP thermal dissolution or that of any other type of aggregation–precipitation process, with good accuracy.

This paper proposes an alternative method for the dynamic study of dissolution processes in alkali halides doped with divalent impurities. It has the advantage of being quicker and more flexible than the classical method which is carried out under quasi steady-state conditions.

Acknowledgments

This work is supported in part by CONACyT and DGAPA-UNAM (México). We gratefully acknowledge grant support by Centro Latino-Americano de Física (CLAF). We also want to thank CYTED-CONACYT for partial support. The authors thank Dr Neil Bruce for revision of the manuscript and Mr R Guerrero for technical assistance.

References

[1] López J, Murrieta H, Hernández J A and Rubio J O 1980 *Phys. Rev.* B **22** 6428
[2] Hernández J A, Cory W K and Rubio J O 1980 *J. Chem. Phys.* **72** 198
[3] Rubio J O, Murrieta H S, Hernández J A and López F J 1981 *Phys. Rev.* B **24** 4847
[4] López F J, Murrieta H S, Hernández J A and Rubio J O 1981 *J. Lumin.* **26** 129
[5] Miyake S and Suzuki K 1954 *J. Phys. Soc. Japan* **9** 702
[6] Miyake S and Suzuki K 1954 *Acta Crystallogr.* **7** 514
[7] Suzuki K 1955 *J. Phys. Soc. Japan* **10** 794
[8] Suzuki K 1958 *J. Phys. Soc. Japan* **13** 179
[9] Suzuki K 1961 *J. Phys. Soc. Japan* **16** 67
[10] Aguilar M G, Rubio J O, López F J, García-Solé J and Murrieta H S 1987 *Solid State Commun.* **44** 141
[11] Murrieta H S, Hernández J A and Rubio J O 1983 *Kinam* **5** 75
[12] Toman K 1962 *Czech. J. Phys.* B **12** 542
[13] Rodríguez F, Gómez Sal J C, Moreno M, De Geyer A and Janot C 1991 *Phys. Rev.* B **43** 7519
[14] Spengler W and Kaiser R 1974 *Phys. Status Solidi* b **66** 107
[15] Bell A G 1880 *Am. J. Sci.* **20** 305
[16] Tam A C 1986 *Rev. Mod. Phys.* **58** 381
[17] Castañeda Guzmán R, Villagrán-Muniz M, Saniger-Blesa J and Pérez-Martinez O 1998 *Appl. Phys. Lett.* **73** 623
[18] Castañeda-Guzmán R, Villagran-Muniz M, Saniger-Blesa J M, Pérez-Ruiz S J and Pérez-Martinez O 2000 *Appl. Phys. Lett.* **77** 3087
[19] Castañeda-Guzmán R, Pérez-Ruiz S J, Villagrán-Muniz M and Saniger-Blesa J 2001 *Anal. Sci.* **17** s122

[20] Pineda Flores L, Castañeda-Guzmán R, Villagrán-Muniz M, Saniger-Blesa J and Huanosta Tera A 2001 *Appl. Phys. Lett.* **79** 1166
[21] Castañeda-Guzmán R, Villagrán-Muniz M, Saniger-Blesa J, Lascano J and Fernández J F 2002 *Ferroelectrics* **273** 333
[22] Navarrete M, Serrania F, Villagrán-Muniz M, Bravo J, Guinovart R and Rodriguez R 2002 *Mech. Adv. Mater. Struct.* **9** 157
[23] Villagrán-Muniz M, Navarrete M and Mejía-Uriarte E V 2003 *Rev. Sci. Instrum.* **74** 732
[24] Rodríguez E, Muñoz J A, Tocho J O and Cussó F 1994 *J. Phys.: Condens. Matter* **6** 10625
[25] Stein J Y 2000 *Digital Signal Processing: a Computer Science Perspective* (New York: Wiley) chapter 9 pp 349–57
[26] Aceituno A P, Cussó F, De Andrés A and Jaque F 1984 *Solid State Commun.* **49** 209